Electronic supporting information for

BINOL blocks as accessible triplet state modulators in BODIPY dyes

Josué Jiménez,[a] Ruth Prieto-Montero,[b] Sergio Serrano,[a] Patrycja Stachelek,[c] Esther Rebollar,[d] Beatriz L. Maroto,[a] Florencio Moreno,[a] Virginia Martinez-Martinez,[b] Robert Pal,[c] Inmaculada García-Moreno,*[,d] and Santiago de la Moya*[,a]

[a] Departamento de Química Orgánica, Facultad de Ciencias Químicas, Universidad Complutense de Madrid, Ciudad Universitaria s/n, 28040, Madrid, Spain. E-mail: santmoya@ucm.es.

[b] Departamento de Química Física, Universidad del País Vasco-EHU, Apartado 644, 48080, Bilbao, Spain.

[c] Department of Chemistry, Durham University, Lower Mount Joy, South Road, Durham DH1 3LE, Durham, United Kingdom

[d] Departamento de Sistemas de Baja Dimensionalidad, Superficies y Materia Condensada, Instituto de Química Física "Rocasolano", C.S.I.C., Serrano 119, 28006 Madrid, Spain. E-mail: i.garcia-moreno@iqfr.csic.es.

Table of contents

1. General methods, instrumentation and techniques

Synthesis

All reagents were used without purification. All solvents were of HPLC grade and were dried according to standard methods. Starting chemical substrates and reagents were used as commercially provided unless otherwise indicated. Thin-layer chromatography (TLC) was performed on silica gel and the chromatograms were visualized using UV light (λ = 254 or 365 nm). Flash column chromatography was performed using silica gel (230-400 mesh) or neutral alumina (activity degree 1, 70-290 mesh ASTM). ^{1}H and ^{13}C NMR spectra were recorded in $CDCl_3$ solution at 20 ºC. NMR chemical shifts are expressed in parts per million (δ scale). ^{1}H and ^{13}C NMR spectra are referenced to residual protons of $CDCl_3$ (δ = 7.26 and 77.16 ppm, respectively) as internal standard. The type of carbon (C, CH, CH_2 or CH_3) was assigned by DEPT-135 NMR experiments. Additionally, complex spin-system signals were simulated by using MestReNova program version 10.0.1-14719. FTIR spectra were obtained from neat samples using the attenuated total reflection (ATR) technique. High-resolution mass spectrometry (HRMS) was performed by using direct sample injection, electrospray ionization (ESI) and hybrid quadrupole time-of-flight mass analyser (QTOF; positive-ion mode was used). Optical rotations in chloroform solution (dye concentration, *c*, expressed in g/100 mL) were recorded at 293 K on an Anton Paar MCP 100 polarimeter.

Spectroscopy

Photophysical signatures were recorded using quartz cuvettes of 1 cm optical path-length and diluted dye solutions (*ca.* $2\cdot10^{-6}$ M) prepared from a concentrated stock solution in chloroform (*ca.* 10^{-3} M), after solvent evaporation under reduced pressure, and subsequent dilution with the desired solvent of spectroscopic grade. UV-vis absorption and fluorescence spectra were recorded on a Varian (model CARY 4E) spectrophotometer and an Edinburgh Instrument spectrofluorimeter (model FLSP 920), respectively. Concentrated dye solutions (mM) were measured using quartz cuvettes with an optical path-length of 0.01 mm and front-face configuration in the fluorescence spectra to avoid reabsorption and reemission phenomena.

Fluorescence quantum yields (ϕ_{flu}) were determined from corrected spectra (detector sensibility to the wavelength) by the optically dilute relative method and by using Eq. S1, where $\int I d\lambda$ is the numerically integrated intensity from the luminescence spectra at the excitation wavelength, A_{exc} is the absorbance at the excitation wavelength, and n is the index of refraction of the solution. The subscripts *R* and *S* denote reference and sample, respectively. PM567 in acetone (ϕ_f = 0.85)[1] was used as the reference.

$$\phi_S / \phi_R = (\int I_S \, d\lambda / \int I_R \, d\lambda)(A_{R,exc} / A_{S,exc})(n_S / n_R)^2 \qquad \text{Eq. S1}$$

The aforementioned spectrofluorometer is also equipped with a wavelength-tunable pulsed Fianium laser. Thus, the Time Correlated Single-Photon Counting (TCSPC) technique was used to record the fluorescence decay curves. Fluorescence emission was monitored at the maximum emission wavelength after excitation by the said Fianium at the maximum absorption wavelength. The fluorescence lifetime (τ) was obtained from the slope of the exponential fit of the decay curve, after the deconvolution of the instrumental response signal (recorded by means of a ludox scattering suspension) by means of an iterative method. The goodness of the exponential fit was controlled by statistical parameters (chi-square, Durbin-Watson and the analysis of the residuals).

Phosphorescence spectra were recorded also in Edinburgh Instrument in low temperature (78 K) by an Optisa DN cryostat and ITC 601 external temperature controller (Oxford Instruments). The phosphorescence lifetime (τ_{pho}) was determined by the time-resolved decay of the phosphorescence signal at 78 K. These long decay curves were measured similarly, in the same spectrofluorometer, but exciting the sample with a 60 W pulsed xenon flash lamp (model µF920H, Edinburgh Instruments), recording the emission at the maximum emission peak and accumulating 5000 counts at the maximum channel. The phosphorescence lifetimes were obtained from the slope following a tail fitting by means of an iterative method by the FAST software. The goodness of the exponential fit was controlled as above described for the fluorescence lifetimes.

Phosphorescence quantum yields at 78 K, ϕ_{pho}, were estimated using Eq. S2, where I_{pho} and I_{flu} are the emission intensity registered at the maximum of the fluorescence and phosphorescence bands respectively, and Φ_{flu}, is fluorescent quantum yield, all them at 78 K.

$$\phi_{pho} / \phi_{flu} = I_{pho} / I_{flu} \qquad \text{Eq. S2}$$

The required Φ_{flu} at 78 K, Φ_{flu}^{78K}, was estimated from the corresponding value at room temperature (Table S1) using Eq S3.

$$\phi_{flu}^{78K} / \phi_{flu}^{rt} = \tau_{flu}^{78K} / \tau_{flu}^{rt} \qquad \text{Eq. S3}$$

Eq. S3 is obtained from Eq S4, assuming that the rate of de-excitation due to fluorescent emission, k_{flu}, does not vary significantly with the temperature.

$$\phi_{flu} = \tau_{flu}\, k_{flu} \qquad \text{Eq. S4}$$

Finally, average lifetime, $<\tau>$, obtained by using Eq. S5, were used in Eq S3, where A is the pre-exponential factor and τ the lifetime of each exponential contribution.

$$<\tau> = \Sigma A_i \tau_i^2 / \Sigma A_i \tau_i \qquad \text{Eq. S5}$$

Quantum yields of singlet oxygen production (ϕ_Δ) were determined by the direct measurement of the singlet oxygen luminescence intensity recorded at 1276 nm (I_Δ) with a NIR detector (InGaAs detector) integrated into a Hamamatsu G8605 spectrofluorometer, by using a 450 W xenon lamp as the excitation source, and 8-methylthio-2,6-diiodoBODIPY(MeSBDP) as the reference (ϕ_Δ = 0.91 in chloroform[2]). The luminescent signals were collected in the 1230-1330 nm range by using a low cut-off filter at 850 nm, and recorded from chloroform solutions (dye concentration between $2.0 \cdot 10^{-6}$ and $1.0 \cdot 10^{-4}$ M) in cells of 1-cm optical path-length, in front-face, 40º and 50º configuration respect to the excitation beam, respectively, and leaned 30º to the plane formed by the direction of incidence. The signals were measured at least by using five different concentrations. Finally, the corresponding singlet oxygen quantum yield (ϕ_Δ) was calculated by using Eq. S6, where *R* and *S* denote reference and sample, respectively; factor $\alpha = 1\text{-}10^{-A}$ corrects the different numbers of photons absorbed by the sample and the reference, respectively, being A the absorbance at the excitation wavelength; and I_Δ is the measured luminescent intensity at 1276 nm.

$$\phi_\Delta = \phi_{\Delta,R} (I_{\Delta,S}/I_{\Delta,R})(\alpha_R/\alpha_S) \qquad \text{Eq. S6}$$

Nanosecond-resolved transient absorption (ns-TA) spectra were recorded on a LP980 laser flash photolysis spectrometer (Edinburgh Instruments, Livingston, U.K.). Samples were excited by a nanosecond pulsed laser (Nd:YAG laser/OPO, LOTIS TII 2134) at 500 nm, operating at 1 Hz and with a pulse width of 7 ns. The transient signals were recorded on single detector (PMT R928P) and oscilloscope for kinetic traces, and ICCD detector (DH320T TE cooled, Andor Technology) for time resolved spectra. Data were analyzed by the LP900 software. Samples with an optical absorbance of 0.3 at the excitation wavelength were deaerated with nitrogen for *ca.* 10 min and measured, aerated for *ca.* 10 min with air and measured, and finally, extra-oxygenated with pure oxygen for *ca.* 10 min and measured. The lifetimes were obtained from the corresponding decay of the long-lived transient band at the absorption maximum at 430 nm, in the presence (aerated and oxygen-saturated solutions) and absence of oxygen (deaerated solution).

Delayed spectroscopy

Aerated solutions at room temperature of the dyes contained in 1-cm optical-path rectangular quartz cells were transversally pumped with intense laser pulses from the second harmonic (532 nm) of a Nd:YAG laser (LOTIS TII, LS-2147) at 10 Hz repetition rate. The time-gated emission upon laser photo-excitation, analyzed perpendicularly to the input radiation, was focused onto a spectrograph (Kymera 193i-A, Andor Technologies) coupled to an intensified CCD camera (iStar, Andor Technologies). This camera enables gate widths ranging from nanoseconds up to seconds, and its opening can be delayed in a controlled way with respect to the incoming pump laser pulse. Neither long-pass filters nor band-pass filters were used to remove the excitation laser since we have verified that these filters, especially long-pass ones, under drastic pump conditions, exhibited its own

fluorescence and/or phosphorescence emission, which could lead to misunderstand the experimental results. Each spectrum is the average of at least 200 scans recorded with a gate time of 50 μs. Delayed emission from the dyes were recorded under experimental conditions well below the threshold for onset their laser action. To meet this requirement, the measurements were carried out at dye concentrations lower than 10^{-4} M. The experiments were usually carried out at excitation energy fluence of 5 mJ/cm^2, which was varied from 1 up to 25 mJ/cm^2 to determine the dependence of the delayed fluorescence on the laser fluence. A solution volume of 3 cm^3 was used in order to avoid (or at least, to reduce) the risk of photo-bleaching the sample during the experiments. This experimental set-up allowed to carry out the projected measurements even under adverse conditions, but avoided to determine properly the efficiency of the delayed emission.

Bioimaging

Mouse Skin fibroblasts (NIH-3T3) cells were maintained in exponential growth as monolayers in F-12/DMEM GlutaMAX™ (Dulbecco's Modified Eagle Medium) 1:1 that was supplemented with 10% foetal bovine serum (FBS) and 1% sodium pyruvate. Cells were grown in 75 cm^2 plastic culture flasks, with no prior surface treatment. Cultures were incubated at 37 °C, 20% average humidity and 5% (v/v) CO_2. Cells were harvested by treatment with 0.25% (v/v) trypsin solution for 5 minutes at 37 ºC. Cells were seeded in 12-well plates on 13 mm 0.170 mm thick standard glass cover-slips and allowed to grow to approx. 50% confluence, at 37 ºC in 5% CO_2. At this stage, the medium was replaced and cells were treated with BODIPY complexes described herein and co-stains as appropriate. For imaging DMEM media (10% FBS, 1% sodium pyruvate) lacking phenol red (live cell media) was used. Following incubation, the cover-slips were washed with live cell media, mounted on slides and the edges were sealed with colourless nail varnish in order to prevent drying out of the sample.

Cell images were obtained using the Leica SP5 II microscope operating with a fiber-coupled 355 nm Coherent laser (Nd:YAG 3rd Harmonic, 80 mW). Leica SP5 II LSCM confocal microscope is equipped with a HCX PL APO 63×/1.40 NA Lambda Blue Oil immersion objective. Data was collected using 2.5× digital magnification at 100 Hz/line scan speed (2-line average, bidirectional scanning) at 488 nm. An Argon (488 nm, 2 mW) laser was used to achieve the 488 nm excitation. Frame size was determined at 1024×1024 pixel.

Cell uptake and co-localization studies were undertaken for dyes **4a** and **4g** using Laser Scanning Confocal Microscope (LSCM) equipped with an incubator allowing strict control of temperature and gas. The cells were dosed (30 μM) with the corresponding dye dissolved in cell grade DMSO for 24 hours prior to imaging. In the cases of **4g**, co-staining experiments using LysoTracker Red verified that this dye is preferably localized in the lysosomes. In the case of **4a** the dye is preferably localized in lipid droplets, as supported by the spherical morphology and high refractive index difference form surrounding cell compartments (evidenced by standard transmission microscopy contrast difference) of the detected subcellular structures.

Time-gated bioimaging experiment was undertaken for dye **4a** with the LSCM by means of adapting the scanning speed and pixels per line. We have managed to generate a quasi-time delay of 1.4 μs. We have obtained this delay scanning between lines at 200 Hz at 1024×1024 pixels. The cells were prepared and incubated according to the method described above.

All images have been recorded using ×63, 1.4 NA Lambda Blue objective on a modified Leica SP5 II confocal microscope as previously described by us.[3]

2. Synthetic procedures and characterization data

Synthesis of 3,3´-disubstituted BINOLs

(*R*)-3,3´-DifluoroBINOL (BINOL: 1,1´-binaph-2-ol) was obtained from (*R*)-BINOL according to the procedure described previously by Zhang *et al*.[4] Characterization data are coincident with the described ones.

(*R*)-3,3´-DichloroBINOL and (*R*)-3,3´-dicyanoBINOL were obtained from (*R*)-BINOL according to the procedures described previously by Tuner *et al*.[5] Characterization data are coincident with the described ones.

(*R*)-3,3´-DiiodoBINOL was obtained was obtained from (*R*)-BINOL according to the procedure described previously by Wu *et al*.[6] Characterization data are coincident with the described ones.

Synthesis of the new BINOL-O-BODIPYs: General procedure

The new BINOL-*O*-BODIPYs were synthesized according to the method we used previously for similar BINOL-*O*-BODIPYs.[7] Thus, a mixture of commercial PM546 (4,4-difluoro-1,3,5,7,8-pentamethylBODIPY, 30 mg, 0.11 mmol, 1 mol equiv.) and aluminum chloride (38 mg, 0.29 mmol, 2.5 mol equiv.) in dry CH_2Cl_2 (6 mL) was placed in a flamed-dry flask and refluxed under argon atmosphere until reaction completion (reaction monitored by TLC). The mixture was cooled down to room temperature and then, a solution of the corresponding 3,3´-disubstituted (*R*)-BINOL derivative (0.23 mmol, 2 mol equiv.) in dry acetonitrile (1.2 mL) was added dropwise. The resulting mixture was stirred at room temperature for additional 6 h, the solvent was removed by distillation under reduced pressure, and the resulting residue purified by flash chromatography to afford the desired product. See Scheme S1.

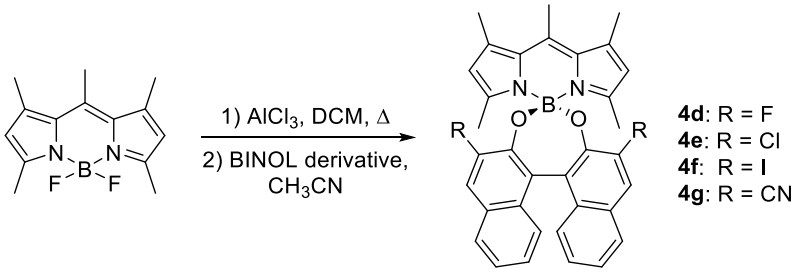

Scheme S1. General synthetic outline.

Synthesis of 4d. According to the described general procedure, commercial PM546 (30 mg, 0.11 mmol) was reacted with (*R*)-3,3´-difluoroBINOL (73 mg, 0.23 mmol). The reaction crude was purified by flash chromatography (neutral alumina, CH_2Cl_2) to obtain **4d** (40 mg, 64%) as an orange solid. R_F = 0.32 (hexane/CH_2Cl_2 1:1). $[\alpha]_D^{20}$ -3221.7 (*c* 0.033, $CHCl_3$). ^{1}H NMR ($CDCl_3$, 300 MHz) δ 7.77 (d, J = 8.1 Hz, 2H), 7.50 (d, $J_{H\text{-}F}$ = 10.7 Hz, 2H), 7.34 (ddd, J = 8.3, 6.5, 0.9 Hz, 2H), 7.19 (dd, J = 8.2, 0.8

Hz,2H), 7.12 (ddd, *J* = 8.3, 6.5, 1.2 Hz, 2H), 5.87 (s, 2H), 2.66 (s, 3H), 2.43 (s, 6H), 1.76 (s, 6H) ppm. ^{13}C NMR ($CDCl_3$, 75 MHz) δ 155.3 (d, $J_{C\text{-}F}$ = 248.1 Hz, C), 154.3 (C), 144.7 (d, $J_{C\text{-}F}$ = 14.7 Hz, C), 141.4 (C), 141.2 (C), 133.6 (C), 130.3 (C), 129.4 (d, $J_{C\text{-}F}$ = 8.8 Hz, C), 127.4 (d, $J_{C\text{-}F}$ = 5.1 Hz, CH), 127.18 (d, $J_{C\text{-}F}$ = 2.0 Hz, CH), 124.6 (d, $J_{C\text{-}F}$ = 2.6 Hz, CH), 124.57 (CH), 123.8 (t, $J_{C\text{-}F}$ = 2.2 Hz, C), 122.3 (CH), 112.2 (d, $J_{C\text{-}F}$ = 18.7 Hz, CH), 17.7 (CH_3), 17.1 (CH_3), 15.3 (d, $J_{C\text{-}F}$ = 1.1 Hz, CH) ppm. FTIR ν 1560, 1506, 1462, 1437, 1400, 1295, 1259, 1187, 1159, 1130, 1107, 983, 964 cm^{-1}. HRMS (ESI$^+$/Q-TOF) *m/z* 545.2220 ([M + H]$^+$; calcd. for $C_{34}H_{28}BFN_2O_2$: 545.2212).

Synthesis of 4e. According to the described general procedure, commercial PM546 (30 mg, 0.11 mmol) was reacted with (*R*)-3,3´-dichloroBINOL (80 mg, 0.23 mmol). The reaction crude was purified by flash chromatography (neutral alumina, CH_2Cl_2) to obtain **4e** (35 mg, 53%) as an orange solid. R_F = 0.57 (hexane/CH_2Cl_2 1:1). $[\alpha]_D^{20}$ -4061.9 (*c* 0.032, $CHCl_3$). ^{1}H NMR ($CDCl_3$, 300 MHz) δ 7.92 (s, 2H), 7.75 (d, *J* = 8.0 Hz, 2H), 7.33 (ddd, *J* = 8.1, 5.6, 2.5 Hz, 2H), 7.17-7.07 (m, 4H), 5.90 (s, 2H), 2.65 (s, 3H), 2.43 (s, 6H), 1.67 (s, 6H) ppm. ^{13}C NMR ($CDCl_3$, 75 MHz) δ 154.4 (C), 150.4 (C), 141.1 (C), 140.9 (C), 133.7 (C), 132.6 (C), 129.6 (C), 128.8 (C), 128.5 (CH), 127.2 (CH), 127.1 (CH), 125.6 (CH), 124.4 (CH), 122.9 (C), 122.6 (CH), 17.8 (CH_3), 17.0 (CH_3), 15.3 (CH_3) ppm. FTIR ν : 1560, 1507, 1186, 1158, 982, 940 cm^{-1}. HRMS (ESI/Q-TOF) *m/z* 577.1628 ([M + H]$^+$; calcd. for $C_{34}H_{28}BCl_2N_2O_2$: 577.1621).

Synthesis of 4f. According to the described general procedure, commercial PM546 (30 mg, 0.11 mmol) was reacted with (*R*)-3,3´-diiodoBINOL (120 mg, 0.23 mmol). The reaction crude was purified by flash chromatography (neutral alumina, CH_2Cl_2) to obtain **4f** (70 mg, 80%) as an orange solid. R_F = 0.45 (hexane/CH_2Cl_2 1:1). $[\alpha]_D^{20}$ -3084.3 (*c* 0.036 $CHCl_3$). ^{1}H NMR ($CDCl_3$, 300 MHz) δ 8.38 (s, 2H), 7.71 (d, *J* = 8.1 Hz, 2H), 7.29 (ddd, *J* = 8.2, 6.7, 1.5 Hz, 2H), 7.11 (ddd, *J* = 8.4, 6.8, 1.5 Hz, 2H), 7.05 (d, *J* = 8.7 Hz, 2H), 5.92 (s, 2H), 2.66 (s, 3H), 2.45 (s, 6H), 1.60 (s, 6H) ppm. ^{13}C NMR ($CDCl_3$, 75 MHz) δ 154.5 (C), 152.8 (C), 141.2 (C), 140.7 (C), 138.8 (CH), 134.0 (C), 133.9 (C), 130.9 (C), 127.1 (CH), 126.9 (CH), 125.9 (CH), 124.1 (CH), 122.7 (CH), 121.2 (C), 95.9 (C), 17.9 (CH_3), 17.0 (CH_3), 15.7 (CH_3) ppm. FTIR ν 1561, 1507, 1411, 1297, 1158, 1131, 980 cm^{-1}. HRMS (ESI/Q-TOF) *m/z* 761.0341 ([M + H]$^+$; calcd. for $C_{34}H_{28}BIN_2O_2$: 761.0333).

Synthesis of 4g. According to the described general procedure, commercial PM546 (30 mg, 0.11 mmol) was reacted with (*R*)-3,3´-dicyanoBINOL (77 mg, 0.23 mmol). The reaction crude was purified by flash chromatography (neutral alumina, CH_2Cl_2) to obtain **4g** (27 mg, 42%) as an orange solid. R_F = 0.15 (hexane/CH_2Cl_2 3:7). $[\alpha]_D^{20}$ -2325.0 (*c* 0.024, $CHCl_3$). ^{1}H NMR ($CDCl_3$, 300 MHz) δ 8.20 (s, 2H), 7.86 (d, *J* = 8.1 Hz, 2H), 7.40 (ddd, *J* = 8.1, 6.9, 1.2 Hz, 2H), 7.25 (ddd, *J* = 8.5, 6.9, 1.4 Hz, 2H), 7.06 (d, *J* = 8.6 Hz, 2H), 5.87 (s, 2H), 2.70 (s, 3H), 2.45 (s, 6H), 1.78 (s, 6H) ppm. ^{13}C NMR ($CDCl_3$,

75 MHz) δ 153.59 (C), 153.57 (C), 142.9 (C), 141.8 (C), 136.0 (CH), 135.3 (C), 134.2 (C), 128.8 (CH), 128.6 (CH), 128.4 (C), 126.8 (CH), 125.1 (CH), 122.2 (CH), 121.4 (C), 117.1 (C), 108.3 (C), 17.6 (CH_3), 17.2 (CH_3), 15.6 (CH_3) ppm. FTIR ν 2229, 1559, 1505, 1474, 1233, 1159, 955 cm^{-1}. HRMS (ESI/Q-TOF) *m/z* 559.2313 ($[M + H]^+$; Calcd. for $C_{36}H_{28}BN_4O_2$: 559.2305).

3. ^{1}H and ^{13}C NMR spectra of new compounds

^{1}H NMR ($CDCl_3$, 300 MHz) of 4d

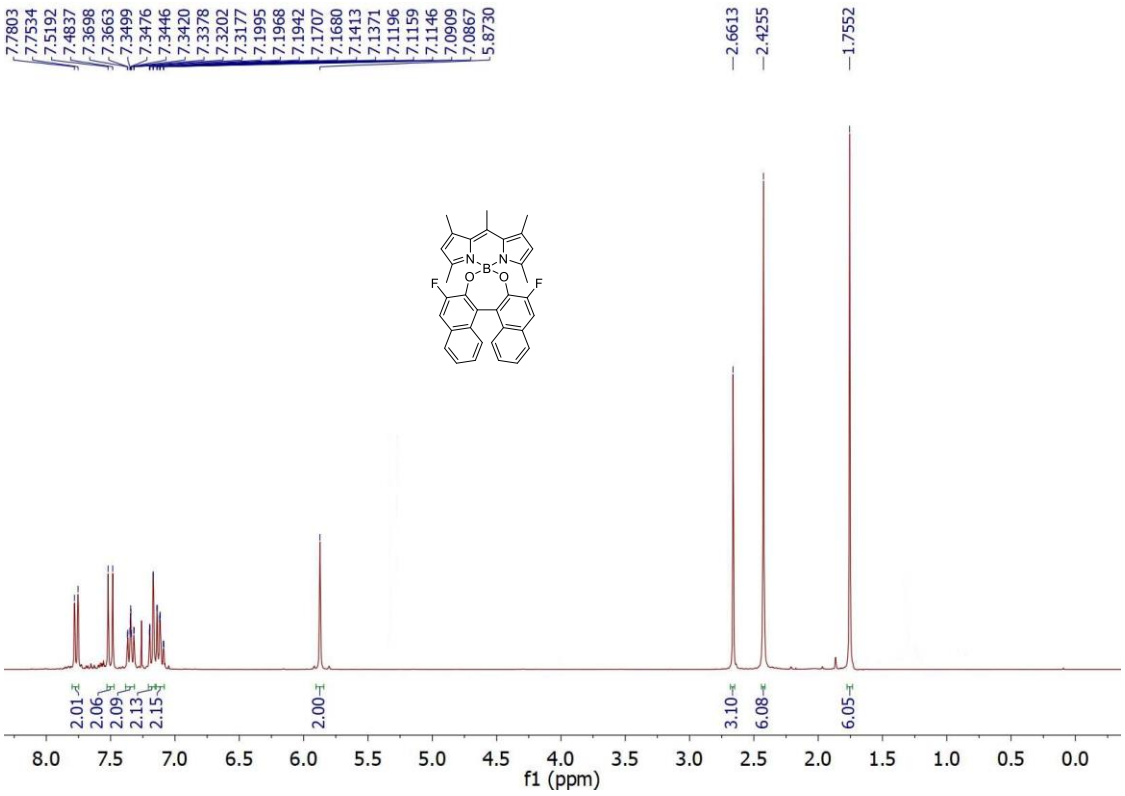

^{13}C NMR ($CDCl_3$, 75 MHz) of 4d

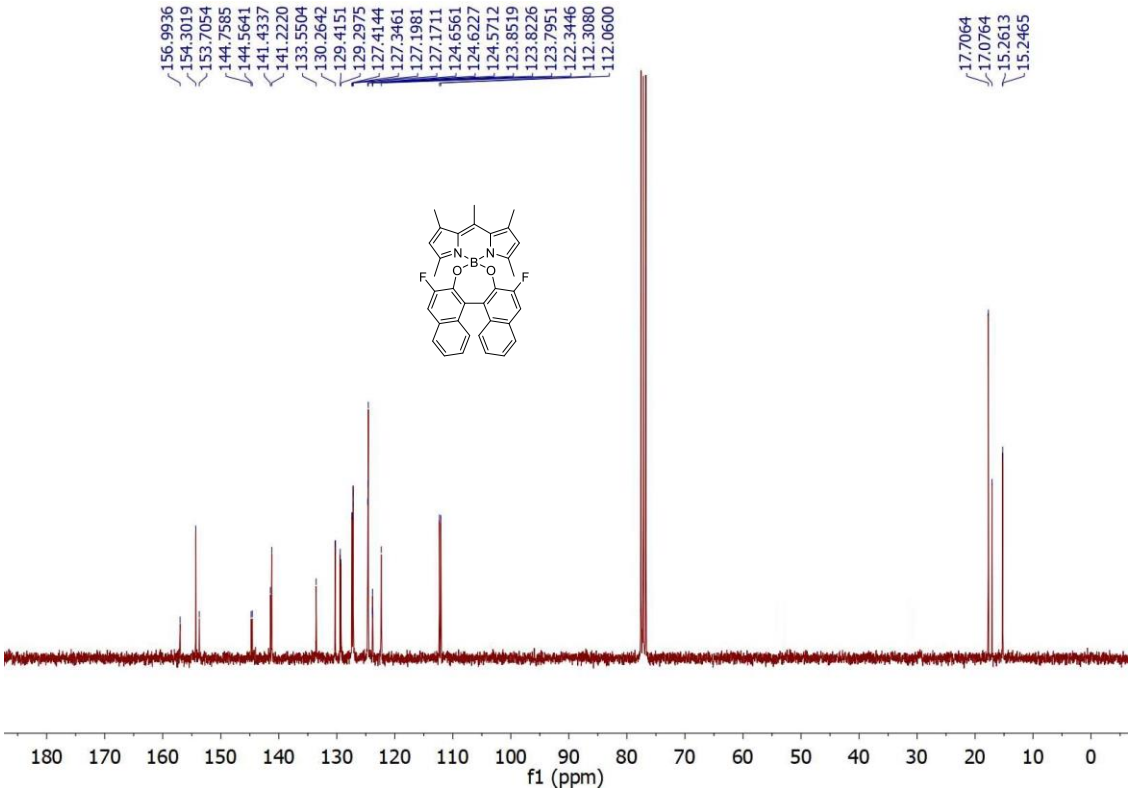

^{1}H NMR ($CDCl_3$, 300 MHz) of 4e

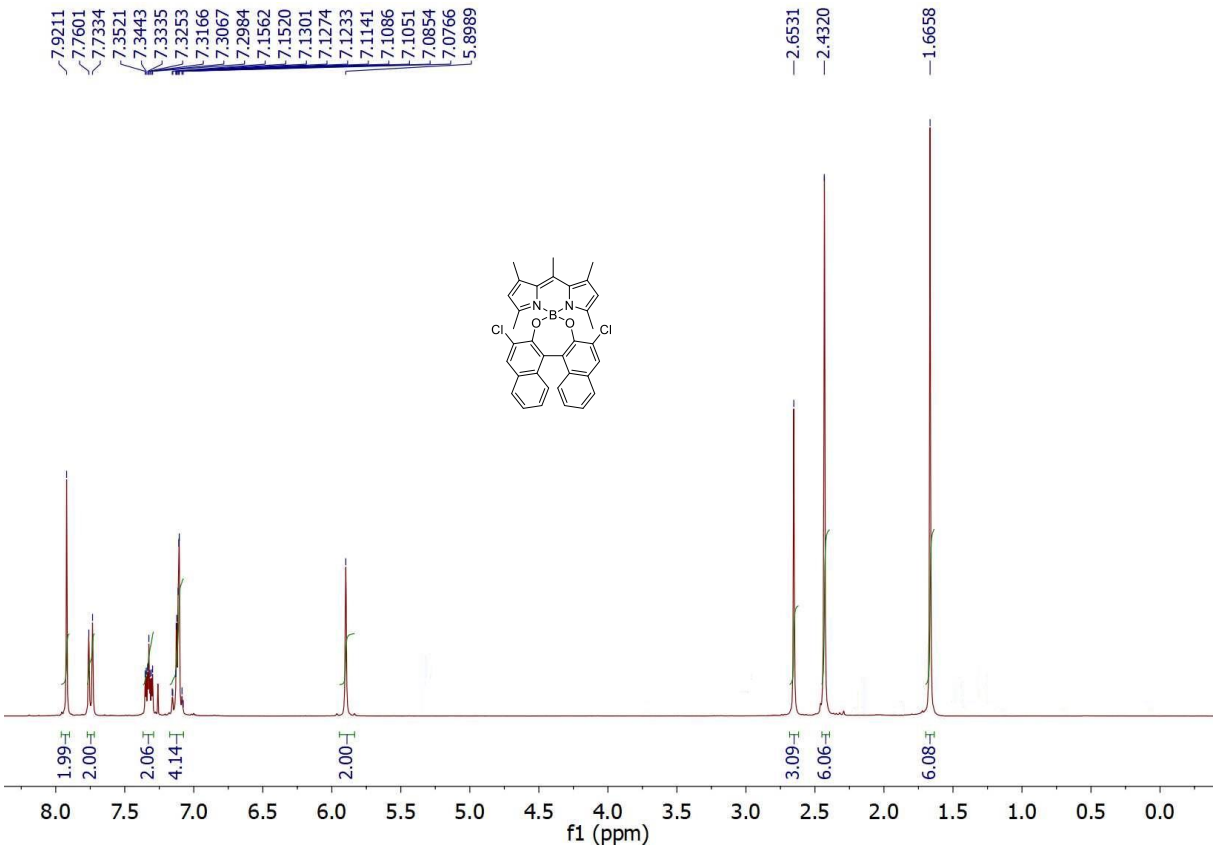

^{13}C NMR ($CDCl_3$, 75 MHz) of 4e

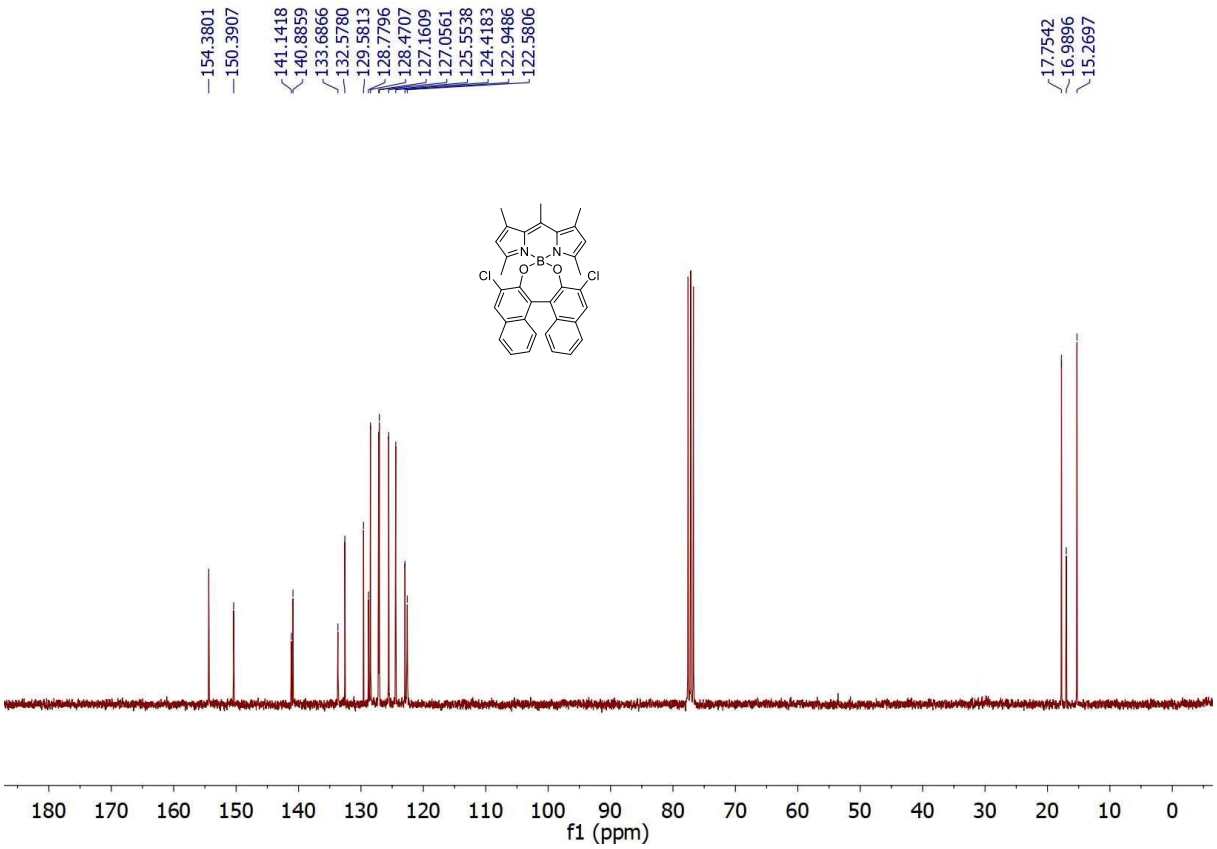

^{1}H NMR ($CDCl_3$, 300 MHz) of 4f

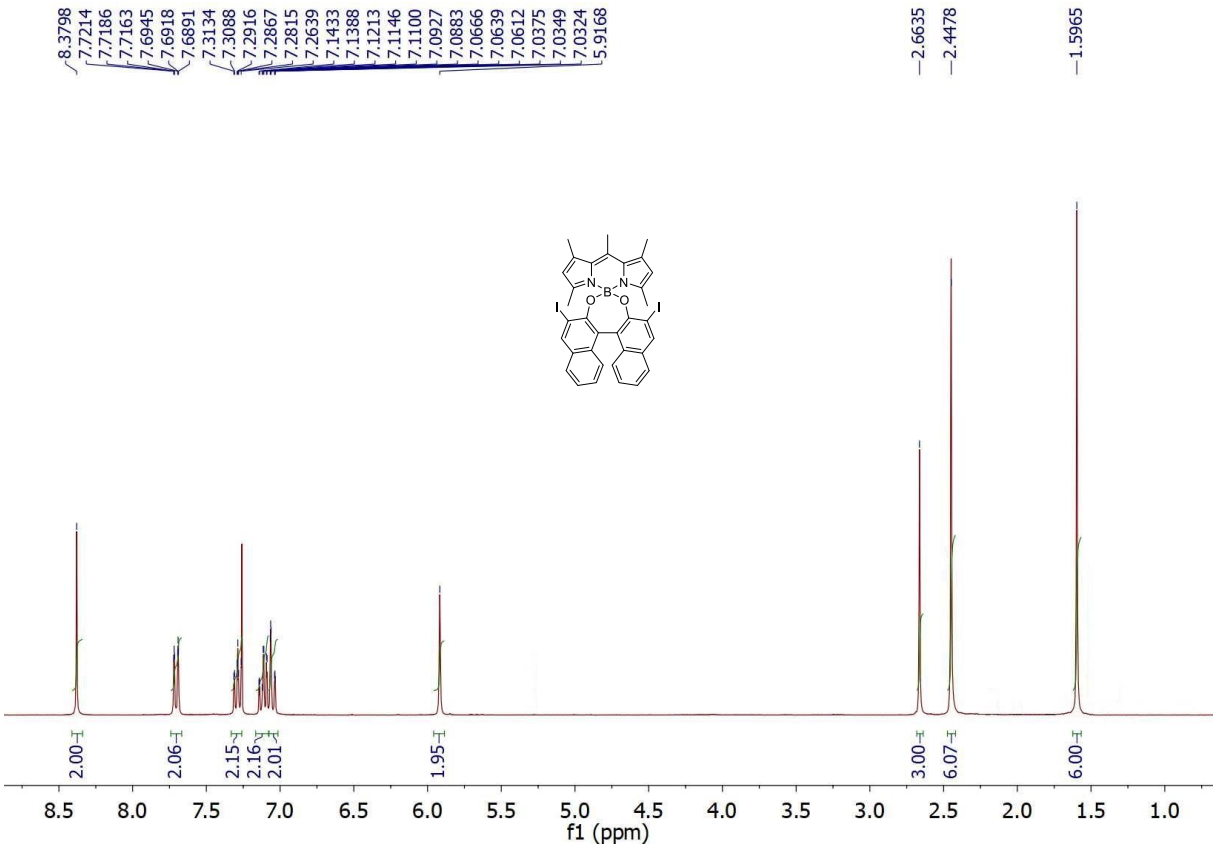

^{13}C NMR ($CDCl_3$, 75 MHz) of 4f

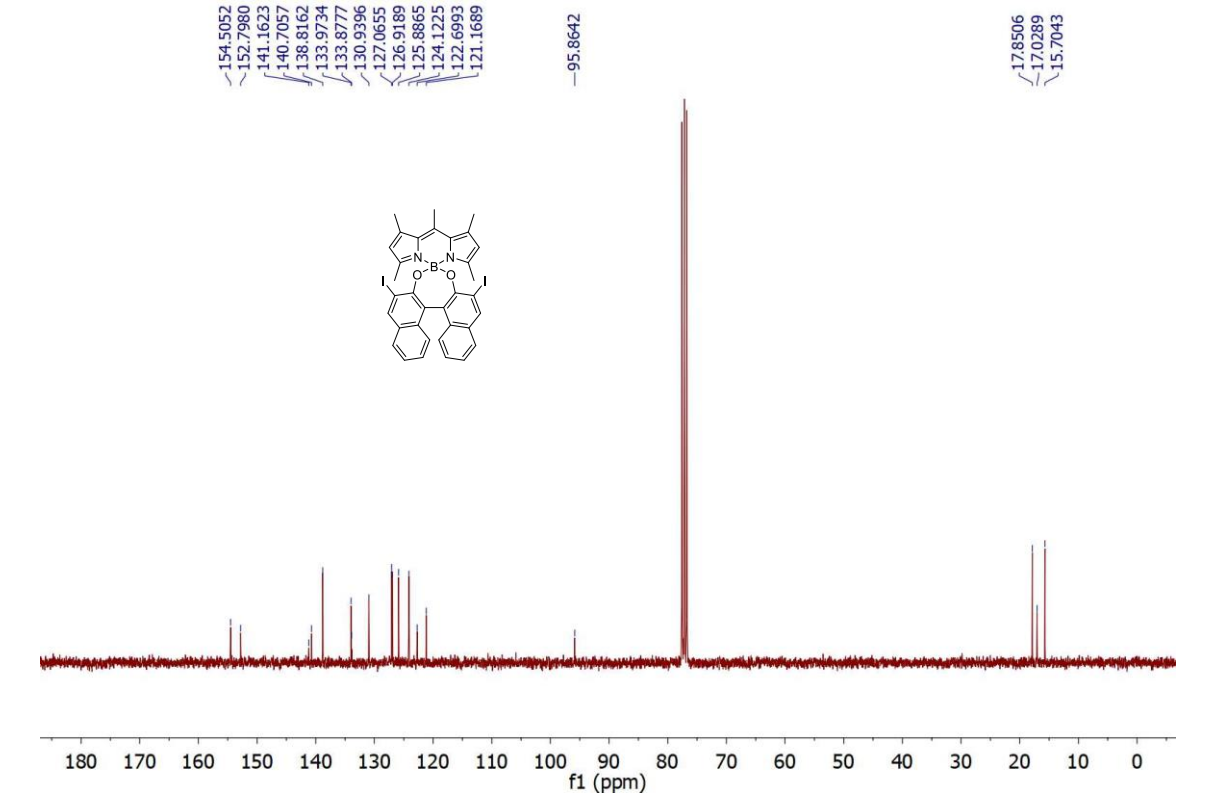

^{1}H NMR ($CDCl_3$, 300 MHz) of 4g

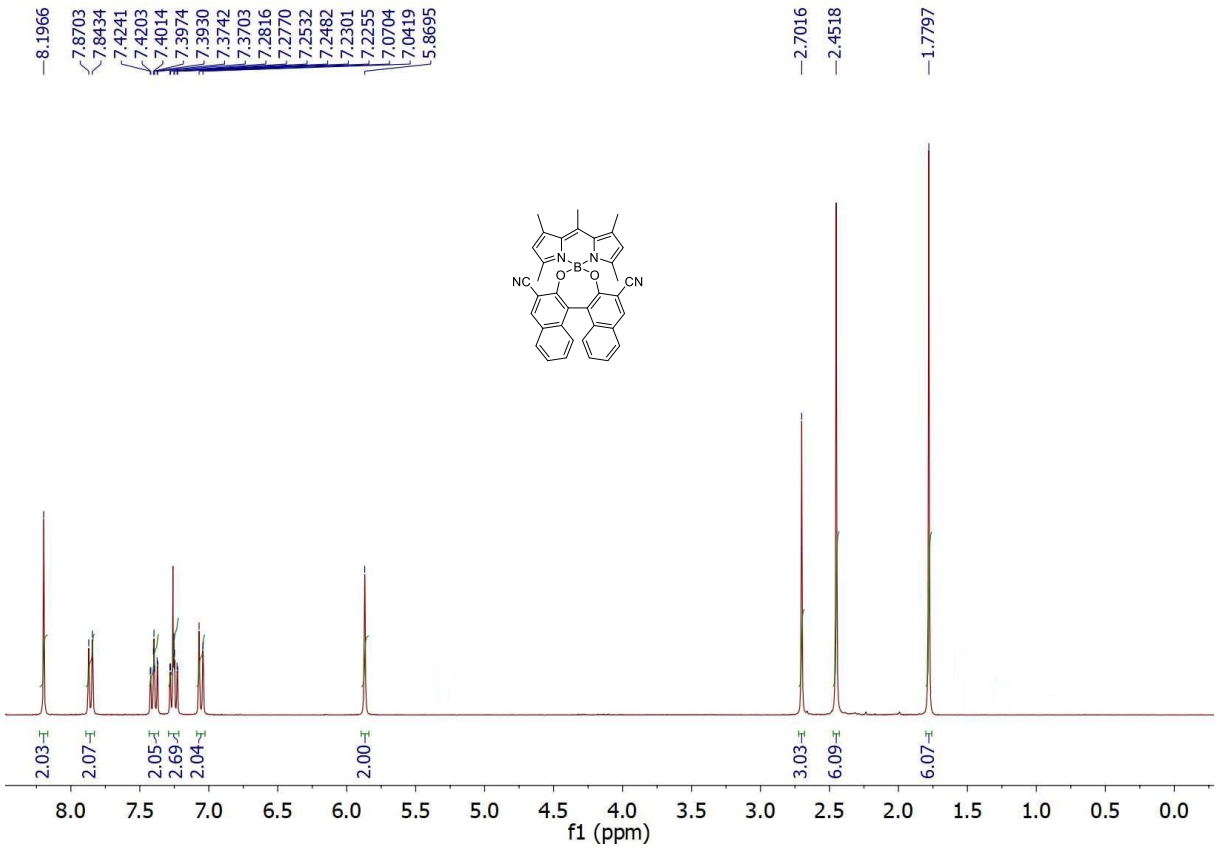

^{13}C NMR ($CDCl_3$, 75 MHz) of 4g

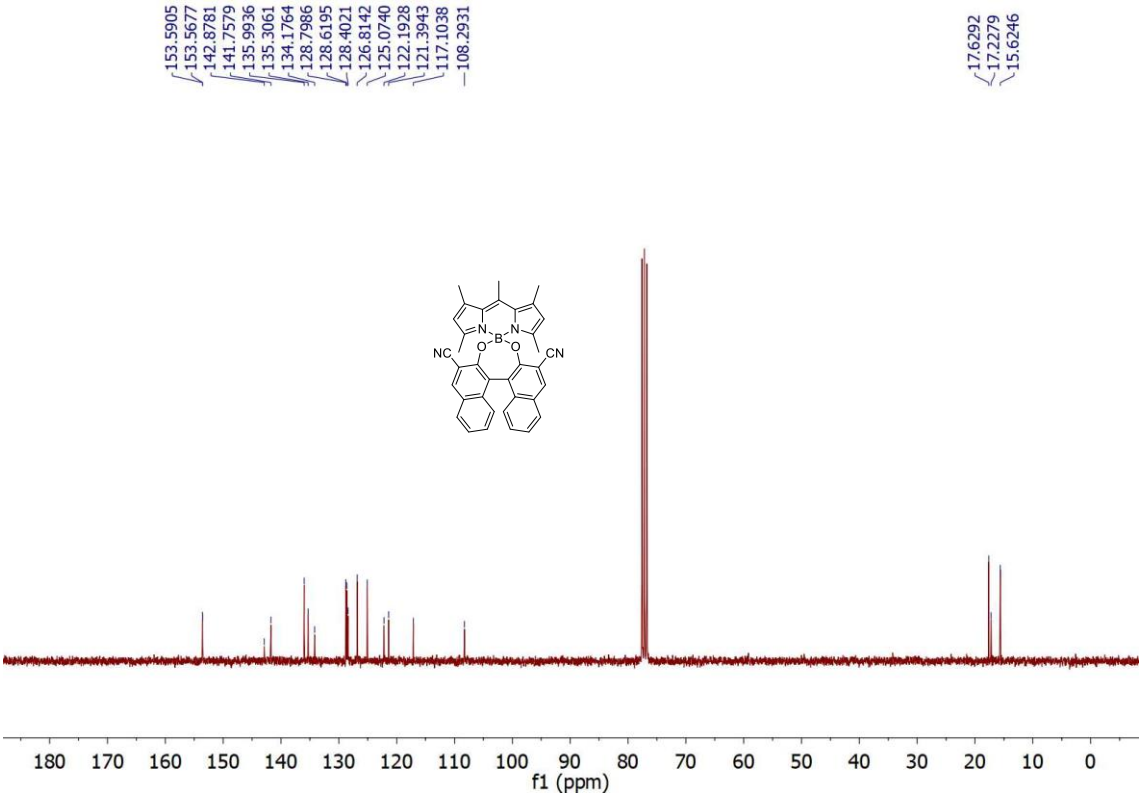

4. Photophysical properties

Table S1. Absorption and fluorescence signatures of BINOL-*O*-BODIPY dyes **4a-g** in diluted solution (2 μM) of different solvents.

dye	Solvent	λ_{ab} (nm)	ε_{max} (10^4 M^{-1} cm^{-1})	λ_{flu} (nm)	ϕ_{flu}	τ_{flu} (ns)
4a[a]	Cyclohexane	505.0	6.9	530.0	0.69	4.93
	Chloroform	503.0	6.6	527.5	0.62	4.26
	Acetonitrile	497.0	6.6	515.5	0.10	0.66 (94%) - 5.36 (6%)
4b[a]	Cyclohexane	502.0	8.2	521.0	0.70	5.44
	Chloroform	501.0	7.3	518.0	0.43	3.22
	Acetonitrile	497.0	6.4	515.5	0.02	0.28
4c[a]	Cyclohexane	502.0	3.4	521.5	0.05	0.44 (97%) - 4.40 (3%)
	Chloroform	501.0	4.1	533.0	0.06	1.19 (11%) - 3.58 (89%)
	Acetonitrile	495.0	3.4	527.5	0.02	-
4d	Cyclohexane	503.0	7.2	535.0	0.70	5.63
	Chloroform	502.0	6.4	522.0	0.67	4.95
	Acetonitrile	495.0	6.0	518.0	0.09	0.63 (96%) - 3.94 (4%)
4e	Cyclohexane	503.0	7.0	526.0	0.89	6.04
	Chloroform	503.0	6.4	522.0	0.82	5.48
	Acetonitrile	496.0	6.2	507.5	0.19	0.66 (75%) - 5.39 (25%)
4f	Cyclohexane	505.0	6.6	530.5	0.19	1.21 (96%) - 5.09 (4%)
	Chloroform	504.0	6.3	529.0	0.12	0.85 (98%) - 4.59 (2%)
	Acetonitrile	498.0	5.3	511.5	0.04	0.22 (95%) - 5.36 (5%)
4g	Cyclohexane	503.0	3.18	522.0	0.88	5.72
	Chloroform	503.0	5.08	529.0	0.87	6.55
	Acetonitrile	495.0	4.62	515.0	0.72	5.70

[a] Data collected from ref. 6.

Table S2: Triplet lifetimes of BINOL-*O*-BODIPY dyes **4a** and **4f** in nitrogen- and air- and oxygen-saturated samples ($\tau^{T}_{N2,}$ τ^{T}_{air} and $\tau^{T}_{O2,}$ respectively).

dye	τ^{T}_{N2} (µs)	τ^{T}_{air} (µs)	τ^{T}_{O2} (µs)
4a [a]	238	0.43	0.085
4f	119	0.52	0.11

[a] Data collected from ref. 6.

Table S3. Fluorescence and phosphorescence signatures of BINOL-*O*-BODIPY dyes **4a** and **4f** at 78 K in deaerated chloroform.

dye	λ_{flu} (nm)	τ_{flu} (ns)	ϕ_{flu}	λ_{pho} (nm)	ϕ_{pho}	τ_{pho} (ms)
4a	515	4.70	0.68	725	0.006	41.9
4f	519	1.24 (80%) - 3.70 (20%)	0.22	725	0.026	3.5 (83%) - 13.2 (17%) [a]

[a] Average lifetime: 7.7 ms, as obtained by applying Eq. S5.

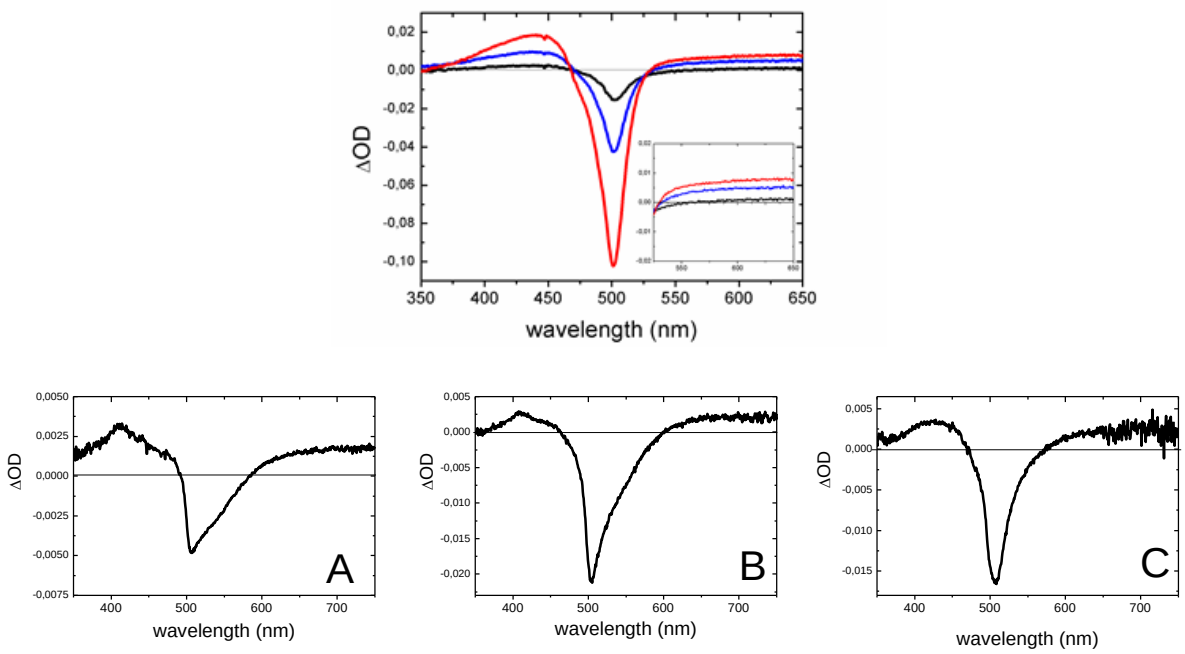

Figure S1. ns-TA spectra of BINOL-*O*-BODIPY **4f** under nitrogen- (up, red), air- (up, blue) and oxygen- (up, black) saturated chloroform, as well as ns-TA spectra of BINOL-*O*-BODIPYs **4d** (down, A), **4e** (down, B), and **4g** (down, C) in deaerated (nitrogen-saturated) chloroform.

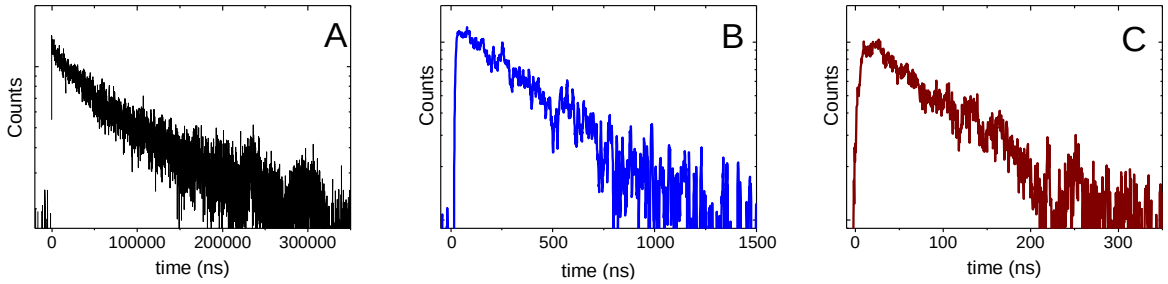

Figure S2. Triplet decay (ns-TA decay) of BINOL-*O*-BODIPY **4f** under nitrogen- (A), air- (B) and oxygen-saturated (C) chloroform.

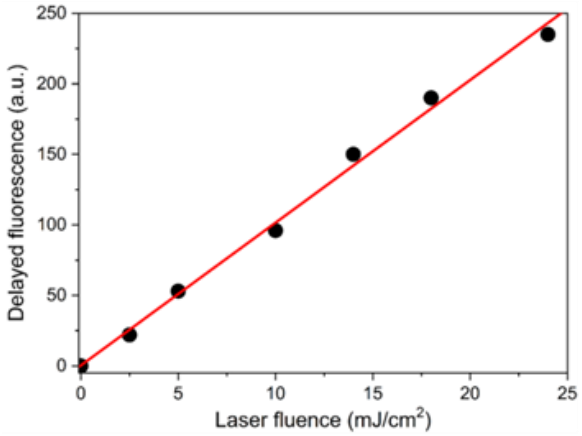

Figure S3. Linear dependency of the delayed emission intensity of BINOL-*O*-BODIPY **4g** on the laser pulse fluence.

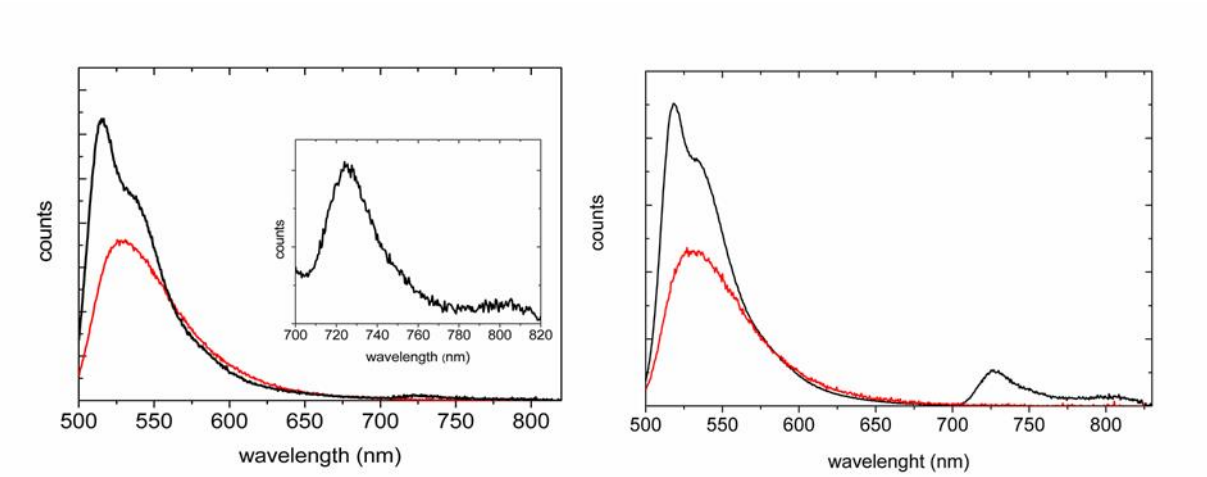

Figure S4. Emission spectra of BINOL-*O*-BODIPYs **4a** (left) and **4f** (right) at room temperature (red) and at 78 K (black) in chloroform upon excitation at 490 nm. Inset: Zoom in of the phosphorescence band of **4a**.

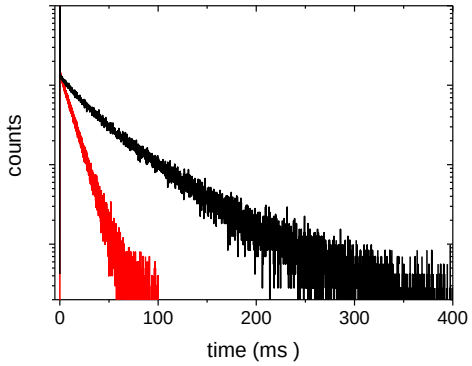

Figure S5. Phosphorescence decay curves of BINOL-*O*-BODIPYs **4a** (black) and **4f** (red) at 78 K, obtained upon excitation at 500 nm and recording the phosphorescence emission at 725 nm.

5. Bioimaging experiments

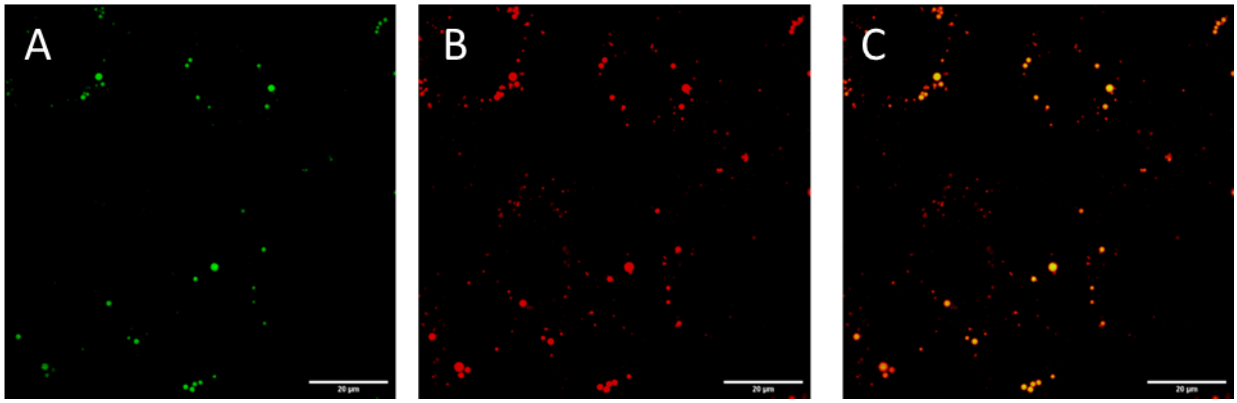

Figure S6. LSCM images of **4g** and LysoTracker Red showing lysosomal localization of **4g** in NIH 3T3 cells. (A) **4g** (λ_{ex} 488 nm, λ_{em} 554-664 nm); (B) LysoTracker Red (λ_{exc} 514 nm, λ_{em} 596-713 nm); (C) RGB merged image verifying co-localization (Pearson´s correlation coefficient, P = 0.76).

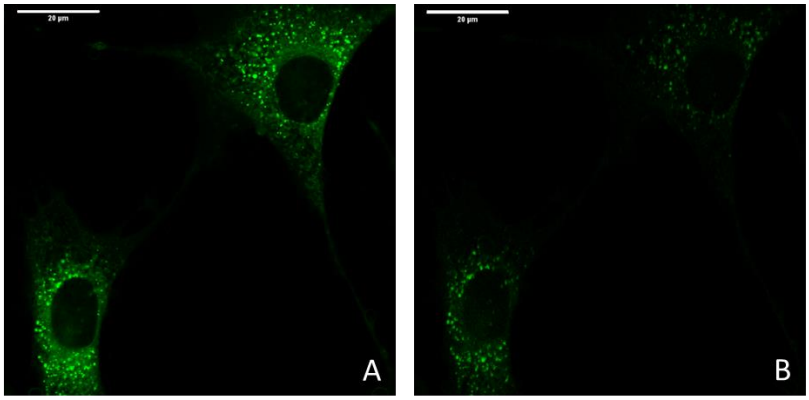

Figure S7. Bioimaging of NIH 3T3 cells by using **4a** without (A) and with (B) 1.4 μs time delay.

6. References

[1] F. López Arbeloa, T. López Arbeloa, I. López Arbeloa, I. García-Moreno, A. Costela, R. Sastre and F. Amat-Guerri, *Chem. Phys.* 1998, **236**, 331-341.

[2] R. Prieto-Montero, R. Sola-Llano ,R. Montero, A. Longarte, T. Arbeloa, I. López-Arbeloa, V. Martínez-Martínez and S. Lacombe, *Phys. Chem. Chem. Phys*. 2019, **21**, 20403-20414.

[3] R. Pal, *Faraday Discuss*., 2015, **177**, 507-515.

[4] Y. Zhang, N. Li, B. Qu, S. Ma, H. Lee, N. C. Gonnella, J. Gao, W. Li, Z. Tan, J. T. Reeves, J. Wang, J. C. Lorenz, G. Li, D. C. Reeves, A. Premasiri, N. Grinberg, N. Haddad, B. Z. Lu, J. J. Song and C. H. Senanayake, *Org. Lett.* 2013, **15**, 1710-1713.

[5] H. M. Turner, J. Patel and N. Niljianskul and J. M. Chong, *Org. Lett.* 2011, **13**, 5796-5799.

[6] T. R. Wu, L. Shen and J. M. Chong, *Org. Lett.* 2004, **6**, 2701-2704.

[7] J. Jiménez, R. Prieto-Montero, B. L. Maroto, F. Moreno, M. J. Ortiz, A. Oliden-Sánchez, I. López-Arbeloa, V. Martínez-Martínez and S. de la Moya, *Chem. Eur. J.* 2020, **26**, 601-605.